Highlights of Collaborations on Metal-Ceramic Interfaces

M. W. Finnis

Atomistic Simulation Group, School of Mathematics and Physics,

The Queen's University of Belfast, Belfast BT7 1NN, Northern Ireland

WWW: http://titus.phy.qub.ac.uk

1 Introduction

The importance of the interaction of metals with oxides is ubiquitous in industry, medicine, transport and the home. Protective aluminium oxide scales are a blessing, iron oxide formation is a curse. Medical implants depend on the adherence and longevity of metal-oxide bonds. We are pursuing a programme of basic research in order to understand better the nature of the bonds involved, which do not fit into the neat categories of ionic, covalent or metallic. The network has supported interactions between the Stuttgart node (M.W.Finnis prior to 1.9.95), Belfast (M.W.Finnis since 1.9.95), Berlin (M. Scheffler), Cambridge (M.C. Payne; also V.Y. Milman now with MSI/Biosym) and Keele (M.J.Gillan). The publications cited below acknowledge this support.

The model system Nb/α-Al_2O_3 was chosen for the first *ab initio* study of a metal-alumina interface in which all atomic positions were relaxed to minimise the total energy. The reasons for this choice were partly experimental. It is an interface which can be prepared to a high degree of perfection at the atomic scale, which has enabled detailed studies by high-resolution electron microscopy. The experimental studies suggested a model of the Nb(111)/α-Al_2O_3(0001) interface which has an intriguing construction. The first two layers of Nb atoms appeared to occupy those sites adjacent to the interfacial plane of oxygen atoms which would have been occupied by Al atoms if the Al_2O_3 crystal structure were extended beyond the interface.

2 Calculations

The calculations, which were done in Stuttgart, are described in detail in our recent publication [1]. We used the pseudopotential/plane wave method developed mainly in the Cambridge group and now commercialised by MSI/Biosym in the form of the CASTEP code. We built on previous experience in the Keele group, where the structure and energies of α-Al_2O_2 surfaces had been

calculated. These calculations were based on a slab of Al_2O_3 containing three layers of oxygen and fifteen atoms altogether, with an equal thickness of vacuum between the (0001) surfaces.

Preliminary calculations were made with a monolayer of Nb replacing the surface layer of Al. Three different symmetry sites for the Nb were investigated, in each case doing a static relaxation of the total energy. Site A is the observed site which continues the bulk lattice, where the Nb sits in a triangular hollow in the oxygen plane, Sites B and C are also triangular hollows, which differ from A by being vertically above an Al atom in an octahedal site within the plane below. The corresponding octahedral site below the A site is empty.

These calculations were followed by adding further layers of Nb, up to eight altogether, filling the gap between the slabs of Al_2O_3. Finally the effect was calculated of replacing the interfacial layer of Nb with Al.

3 Results for Nb/α-Al_2O_3

The monolayer calculations showed that when Nb is in site A the energy of the system is lowest. In this case the relaxations of the atomic positions are also very small. By contrast, sites B and C are much higher in energy, by more than 3eV, and the relaxations are very pronounced. We observe that when the Nb is on sites B and C there is a strong repulsion between it and the Al atom below it. This is an ionic repulsion. We showed this by plotting the charge density for different energies, which revealedf that the Nb is in the form of an Nb^{3+} ion, a non-spherical ion with an occupied d-orbital perpendicular to the surface.

With five to eight layers of Nb in a multilayer configuration the situation is rather different. There is still charge transfer to the surface layer of oxygen, enabling it to have a full shell of p-electrons. However, the second layer of Nb participates in this bonding too. The overlap of the Nb d-band with the oxygen 2p-band gives rise to a strong hybridisation which does not happen in the monolayer case. Details of the electronic structure are altered very significantly within the Nb even four layers from the interface; notably there is a prominent resonance above the Fermi energy. The Fermi energy itself lies 3eV above the top of the valence band, about half the distance found with the self-consistent tight binding approach. This result is similar to that of other workers who have made calculations on interfaces of Ag, Ti and Al on MgO, in which the Fermi energy is 2.0-2.3eV above the top of the valence band in each case.

The Nb layers at the interface relax quite strongly as a result of the competition of the first two layers of Nb for bonding with the oxygen. The first two layers of Nb pinch together by 0.04nm compared to their bulk spacing. This is just within range of what should be detectable by high resolution transmission electron microscopy, but it has not yet been investigated at the required resolution. When we replace the interfacial layer of Nb by Al, the relaxation is much reduced - it is as if the second Nb layer has given up the competition for O in the presence of the more electropositive Al.

From our predicted atomic positions our colleague G. Moebus in Stuttgart was able to simulate electron microscope images. A surprising result of this was that the difference between an Al-terminated and an O-terminated interface would only just be within the limit of experimental detection by this technique. Other methods, however, such as electron energy loss spectroscopy have been applied which strongly suggest that the Nb termination is the actual one (J. Bruley,

private communication).

4 Conclusions and other issues

We have demonstrated the usefulness of pseudopotential calculations for studying metal-ceramic interfaces. The nature of the bonding is complicated and different for a monolayer and a multilayer. Relaxations of the atomic positions, especially in metastable equilibrium geometries, can be very large. The results of this collaboration are set in the context of other theories and models of metal-ceramic bonding in ref. [2].

A frequently asked question has been whether we could predict which of the interfaces between Nb(111) and Al_2O_3(0001) would be more stable, the Nb terminated or the Al terminated one. The answer is yes, in principle we could, but the answer depends on the chemical potentials of the species involved, so it depends on the amount of Al or O dissolved in the Nb. Issues of chemical equilibrium are involved here, which will probably have a bigger role to play in future calculations which attempt to use the elementary energies provided by *ab initio* methods to build a thermodynamic model. Of course, in practice one is not always dealing with the thermodynamically stable structure of an interface, for example if it is prepared at relatively low temperature by molecular beam epitaxy.

Another issue is to try to find simpler models which describe either the atomic interactions or the electronic structure of such interfaces. Real interfaces involve imperfections, defects and roughness, which must affect adhesive energies and other properties. However, with our *ab initio* methods the simulation of all but very simple, atomically flat and coherent, systems is too computationally demanding and there will always be problems for which this remains the case. With a view to tackling such problems, a simple classical interatomic force model has been studied, based on the image interaction between an ion and a metallic surface. Within the framework of the Network we compared the results of this model with *ab initio* calculations for a single external point charge above three low index Al surfaces, and found that it gives a very good account of the differences due to the different corrugations in each case [3]. Work to test and apply it to interfaces is in progress. This work will go hand in hand with detailed *ab initio* calculations of the ideal work of adhesion, which was not addressed in the Nb/Al_2O_3 studies reported here.

References

[1] C Kruse, MW Finnis, JS Lin, VY Milman, MC Payne, A De Vita and MJ Gillan, First principles study of the atomistic and electronic structure of the Niobium/α-Alumina(0001) interface, *Phil. Mag. Lett.* **73** 377-383 (1996).

[2] MW Finnis, Review article: The theory of metal ceramic interfaces, *J. Phys.: Condens. Matter* **8** 5811-5836 (1996).

[3] MW Finnis, R Kaschner, C Kruse, J Furthmüller and M Scheffler, The interaction of a point charge with a metal surface: theory and calculations for (111), (100) and (110) aluminium surfaces, *J. Phys.: Condens. Matter* **7** 2001-2019 (1995).

Highlights of Vienna-Zürich Collaboration

Electric Field Gradients using the Projector Augmented Wave Method

H. Petrilli*, P.E. Blöchl *(IBM Research Division, Zürich Research Laboratory)*
K. Schwarz, P. Blaha *(Technical University Vienna)*

Mössbauer experiments and resonance techniques probe quantities such as hyperfine splittings and electric field gradients (EFG), that are sensitive to the local environment of atoms in molecules or solids. Combined with electronic structure calculations, which predict such quantities, these experiments yield most valuable information on the atomic structure and provide a viable test of the approximations underlying electronic structure calculations.

As the measured properties reflect the density in the immediate neighborhood of the nucleus the common pseudopotential approach cannot make such predictions other than through indirect reconstruction techniques. Also the demands on all-electron electronic structure methods are extreme, as the EFGs are dominated by the density in a region that affects the total energy only to a small extent. Currently, the full-potential LAPW method, as used by the Vienna group, is considered most realiable for EFG calculations.

We have now applied the Projector Augmented Wave (PAW) method for the first time to EFG calculations. This work has two goals. First, we hope to extend the range of applications to a wider class of systems by exploiting the flexibility of the PAW method. Secondly, by comparing the results of two independent electronic structure methods, we hope to predict the result for a given density functional independent of numerical errors. This is a nontrivial task, because EFGs have proven to be extremely sensitive to numerical approximations, and variations of up to ten percent are not uncommon.

As a first step we applied our new approach to thirteen different systems including solids and molecules, containing main group elements and transition metal elements. The results have been compared to experiment and LAPW calculations. Our calculations reproduce experiment with an average error of fifteen percent, which is comparable with the experimental error bar. The comparison with LAPW shows an average error of less than ten percent.

Supported by grants from the Swiss Federal Office for Education and Science; BBW Nr. 94.028.
* permanent address: Universidade de Sao Paolo; CP 66318; 05389-970 Sao Paolo, SP; Brasil

Diffusion and Defects using the Projector Augmented Wave Method

J.Sarnthein, K. Schwarz *(Technical University Vienna)*
P.E. Blöchl *(IBM Research Division, Zürich Research Laboratory)*

Li_3N is a superionic conductors with a very high Li conductivity. The diffusion and consequently the conductivity in Li_3N shows a significant anisotropy parallel and perpendicular to the c-axis of the hexagonal structure. In order to understand the microscopic nature of the conductivity we investigated the defects and diffusion by ab-initio molecular dynamics studies using the Projector Augmented Wave (PAW) method.

The barrier for lithium jumps to vacant adjacent sites in the Li_2 plane was found to be very small, namely 0.004 eV, whereas jumps perpendicular to this plane have a barrier of 0.58 eV. Therefore diffusion in the plane is limited by the formation of vacancies, whereas perpendicular to the plane (i.e. parrallel to the c axis) the barrier dominates. A molecular dynamics run at 800 K using the Projector Augmented Wave (PAW) method confirms the anisotropy of diffusion and leads to diffusion coefficients consistent with experiment. From the trajectories of the molecular dynamics run we deduce a microscopic diffusion mechanism and find that mainly isolated rather than correlated jumps take place.

1. J.Sarnthein, K.Schwarz and P.E.Blöchl: Ab-initio molecular dynamics study of diffusion and defects in Li_3N. Phys.Rev.B **53**, 9084-9091 (1996)

Highlights of Rennes-Zürich Collaboration

Ab-initio calculations of 1-Dimensional band-structures of mixed-stack molecular compounds: Tetrathiafulvalene-p-benzoquinones derivatives

C. Katan, C. Koenig and P. E. Blöchl*
Groupe Matière Condensée et Matériaux, Université Rennes-1, Campus de Beaulieu, 35042 Rennes-Cedex, France
**IBM Research Division, Zürich Research Laboratory, CH-8803 Rüschlikon, Switzerland*
(Rennes-Zürich Collaboration)

Mixed-stack organic charge-transfer compounds are composed of two types of flat molecules: closed-shell-π electron donors (D) and acceptors (A), which are stacked into linear chains. Members of this class undergo structural phase transitions under pressure, temperature or photoirradiation. Common to all these transitions is the loss of inversion symmetry resulting in a "dimerization" of the chains into D–A pairs. Simultaneously, a more or less abrupt change in the charge transfer is observed.

In the past ten years, these transitions have been studied using 1D models based primarily on Hubbard-like Hamiltonians or free-energy expansions. Qualitatively different transitions can be reproduced within these models by interplay of different parameters, which are usually extracted by fittings to the experimental data.

Recently, first-principles calculations for these systems have become possible, providing the means to determine *ab-initio* values for these parameters and explore the validity of the model assumptions, and thus to arrive at reliable material-specific predictions. We have performed the first ab-initio calculation of the electronic-structure of TTF-CA and TTF-2,5Cl_2BQ. The method used is the projector augmented wave (PAW) method, within the gradient corrected local approximation of the density functional theory.

We first analyzed the electronic and dynamical properties of isolated molecules of TTF, CA and 2,5Cl_2BQ [1]. We provided thus the first theoretical confirmation of the linearity of the variation of some intra-molecular vibrations with ionicity, which is assumed by the experimentalists for the determination of the inter-molecular charge transfer.

Then we investigated the 1D properties of the high symmetry phase of these compounds [2], in order to understand the microscopic nature of the intra-chain coupling between the molecules. Our results led to a visualization at an atomic scale of these interactions and showed especially that, contrary to what has been assumed up to now in 1D model-Hamiltonians, the hybridization between the crystalline states is maximum at the border of the Brillouin zone and not at the Γ point.

In the frame of a 1D tight binding model, these interactions can be expressed by hopping integrals with alternating signs along the chains. Ab-initio values for these integrals and for the charge transfer have been determined from the calculated dispersion, and a clear understanding, at a microscopic level, of the tight relation between symmetry breaking and charge transfer increase has been obtained.

The qualitative features of the 1D behavior result from rather general symmetry arguments. This applies to the entire series of mixed-stack tetrathiafulvalene-p-benzoquinones halogen derivatives. Hence, the large variety of phase transitions in this class of materials must be rooted partly in the different donor and acceptor strengths and partly in the three-dimensional interactions between the chains, which differs greatly from one compound to another. Studies of those interactions are in progress.

References

[1] C. Katan, P.E. Blöchl, P. Margl and C. Koenig, Phys. Rev. B **53**, 12112 (1996).

[2] C. Katan, P.E. Blöchl and C. Koenig, IBM Research Report RZ 2879 (1996), submitted.

Highlight of the results obtained by the Lisbon-Antwerp collaboration

Structural Optimization of Ternary Calcium Nitrides

P.E. Vansant, P.E. Van Camp, V.E. Van Doren
University of Antwerpen (RUCA), Dept. of Physics,
Groenenborgerlaan 171, B-2020 Antwerpen, Belgium
J.L. Martins, I. Souza
INESC, Rua Alves Redol 9, P-1000 Lisboa, Portugal;
Instituto Superior Tecnico, Avenida Rovisco Pais 1, P-1096 Lisboa, Portugal

An optimization scheme for crystal structure parameters developed recently by Souza and Martins was applied to the study of ternary calcium nitrides. The forces and stresses were calculated with a local-density pseudopotential plane wave method using an iterative matrix diagonalization scheme. The enthalpy at a given pressure is then minimized with respect to the atomic coordinates as well as with respect to the cell metric.

We calculated the zero pressure structure parameters of the perovskite structure Ca_3BiN and of the distorted perovskite structures Ca_3PN and Ca_3AsN. For Ca_3BiN the crystal has cubic symmetry, but for Ca_3AsN and Ca_3PN the crystal has an orthorhombic symmetry with four formula units per cell. The calculated lattice constants shown in the table are in excellent agreement with experiment (values in parenthesis).

The dependence on pressure of the structural parameters of Ca_3AsN was also investigated. We found the orthorhombic symmetry of Ca_3AsN has still a lower enthalpy then the cubic symmetry of Ca_3AsN even when the pressure increases.

Joint Publications:

"Structural Phase Transformations of Aluminum Arsenide". P. E. Van Camp, V. E. Van Doren and J. L. Martins, "Proceedings of the 22nd International Conference on The Physics of Semiconductors", edited by D. J. Lockwood, Vol. 1, p. 181 (World Scientific, Singapore, 1995).

Crystal	a (Å)	b (Å)	c (Å)
Ca_3BiN	4.862		
	(4.888)		
Ca_3AsN	6.720	6.715	9.526
	(6.725)	(6.720)	(9.534)
$Ca_3P\ N$	6.710	6.659	9.453
	(6.709)	(6.658)	(9.452)

Table 1: Calculated and measured (in parenthesis) lattice constants of ternary nitrides.

"High Pressure Properties of the Alkaline-Earth Sulphides". P. E. Van Camp, V. E. Van Doren and J. L. Martins, Phys. Stat. Sol. (b) **190**, 193 (1995).

"Electronic Structure and Pressure Dependence for some Ternary Calcium Nitrides". P. R. Vansant, P. E. Van Camp, V. E. Van Doren and J. L. Martins, Phys. Stat. Sol. (b) **198**, 87 – 91 (1996).

"High Pressure Phases of Magnesium Selenide and Magnesium Telluride". P. E. Van Camp, V. E. Van Doren and J. L. Martins, Accepted for publication in Phys. Rev. B, Issue of 1 January 1997.

"Structural Optimization of Ternary Calcium Nitrides" P. R. Vansant, P. E. Van Camp, V. E. Van Doren and J. L. Martins, in preparation.

Highlights of Athens–Jülich Collaboration

Towards an ab-initio study of dynamical properties of materials: Calculating forces and lattice distortions

N. Papanikolaou[†], N. Stefanou[†], R. Zeller[‡], P.H. Dederichs[‡]

[†]*University of Athens, Section of Solid State Physics, Panepistimioupolis, GR-15784 Athens, Greece*

[‡]*Institut für Festkörperforschung, Forschungszentrum Jülich, D-52425 Jülich, Germany*

The theoretical methods for the study of materials have enormously advanced in recent years. With the help of modern computers we are now able to simulate the microscopic behavior of real materials from first principles and predict experimentally observed properties with a high accuracy. The Korringa-Kohn-Rostoker (KKR) Green function method, which is based on multiple-scattering theory, is a powerful tool to calculate the electronic structure of solids. One of the most important and challenging problems for today's electronic structure methods is the study of the dynamical properties and the diffusion processes in solids. A key issue in such a study is the accurate calculation of the atomic forces. Within the framework of the Jülich-Athens collaboration we have extended the KKR Green function method to calculate reliably the inter-atomic forces and treat lattice relaxation effects. The calculations rely on an exact treatment of the anisotropic potential in each cell, leading to a set of coupled radial equations which are solved iteratively. As a benefit of the full potential KKR-method the forces can be calculated by the Hellmann-Feynmann theorem, since the Pullay corrections vanish.

Using this method we have firstly studied the local lattice distortion around impurities in metals [1,2,3]. For the case of 3d impurities in Cu [1] we found relatively small relaxations of the neighboring atoms, which practically do not effect the local magnetic moments. The results for the local relaxations are in very close agreement with EXAFS measurements, while the predicted volume changes of the dilute alloys agree very well with lattice parameter measurements. The good agreement is however only obtained, if the semi-core states of the impurities are treated as valence states, which is particularly important for the early transitions metal impurities. Calculations for 3d impurities in Al yield a qualitatively different picture, i.e. large relaxations and a drastically increased relaxation energy. Our calculations resolve the long standing problem of the existence or non-existence of a local magnetic moment of 3d impurities in Al [2]. Contrary to the experiment where no local moment was observed for an Fe impurity in Al, previous theoretical calculations predicted a moment of about 1.5 μ_B on the Fe site. This discrepancy was resolved when lattice distortion around the Fe impurity was correctly incorporated into our calculations which then show that the Fe magnetic moment vanishes in the ground-state configuration. We also find that the lattice relaxation is important for the magnetic properties of other impurities, e.g. the magnetic moment of Cr and Mn in Al is strongly reduced. At present we are applying the same method to defects in semiconductors. Here we study the complicated structure of defect complexes and their hyperfine properties which are strongly affected by relaxations.

The success of our method to deal with the lattice distortion has initiated preliminary studies of the lattice dynamics of metals. By shifting one atom and calculating the forces on the neighboring ones, the Born-von Karman coupling parameters can be calculated directly in real space. Calculations of the phonon spectra of several fcc metals are now in progress and give encouraging results. One of our main future aims is the study of structural distortions on surfaces, where these phenomena, due to the more open structures, are more important. Such an extension will allow us to study the relaxations and dynamics of ideal surfaces, as well as surfaces with single adsorbate atoms or small clusters.

One of the main benefits of the Athens-Jülich collaboration was the possibility offered to a young scientist from Greece, N. Papanikolaou, to work in Jülich as a postdoc during 1996 within the TMR-Network "Interface Magnetism".

REFERENCES

[1] N. Papanikolaou, R. Zeller, P.H. Dederichs, and N. Stefanou, Phys. Rev. B (in press)

[2] N. Papanikolaou, R. Zeller, P.H. Dederichs, and N. Stefanou, Comp. Mat. Sci. (submitted)

[3] N. Papanikolaou, N. Stefanou, R. Zeller, and P.H. Dederichs, "Stability of Materials", NATO ASI, A. Gonis, P.E.A. Turchi and J. Kudrnovsky, eds. Plenum Publ. Corp., New York 1996 p.419-424

Highlights of Aarhus-Daresbury-Karlsruhe Collaboration

Rare Earth Materials studied with the Self-Interaction Corrected Local-Spin-Density Approximation

A. Svane[a], Z. Szotek[b], W.M. Temmerman[b], J. Lægsgaard[a],

S.V. Beiden[c], H. Winter[d] and G. Gehring[c]

[a] *Institute of Physics and Astronomy, University of Aarhus,*

DK-8000 Aarhus C, Denmark

[b] *Daresbury Laboratory, Warrington WA4 4AD, United Kingdom*

[c] *Department of Physics, University of Sheffield,*

Sheffield S3 7RH, United Kingdom

[d] *Forschungszentrum Karlsruhe, INFP, Postfach 3640, Karlsruhe, Germany*

The electronic structures of rare earth compounds are investigated using the self-interaction corrected (SIC) local-spin-density (LSD) approximation to density functional theory implemented with the *ab-initio* linear-muffin-tin orbitals (LMTO) band structure method. This scheme allows a treatment of the rare earth f–electrons as either localized or delocalized, and provides a framework for discussing the phase transitions occurring as the f–electrons change from being predominantly localized to predominantly itinerant as a function of applied pressure. The present collaboration has joined the efforts to: (a) apply the SIC-LSD formalism to more compounds and (b) improve the present computer codes. The current implementations are discussed in Refs. [3,5] below, while recently an extension to a fully relativistic description has been implemented, and the first results are being written up (Ref. [7]).

For cerium metal it is found [1-3] that the two fcc-phases, the low volume α– and the high-volume γ–phase, may well be described by the method, when the f–electrons are treated as delocalized or localized, respectively. The total energy is almost the same in these two phases, in agreement

with the experimental fact that transitions between them are observed at moderate changes in temperature or applied pressure. The volume collapse of $\sim 23\%$ is somewhat too large compared with the $\sim 15\%$ observed experimentally, which primarily is caused by a too small theoretical lattice constant for the α–phase. By a simple thermodynamic extension the phase diagram of cerium may qualitatively be reproduced, including the occurrence of a critical point [3].

The cerium monopnictides CeN, CeP, CeAs, CeSb and CeBi exhibit a series of structural phase transitions with accompanying large volume changes, which all may be explained [4-6] by the competitions between the f–electrons being either localized or delocalized and between the B1 and B2 (i.e., the NaCl and CsCl) crystal structures. All crystallize in the B1 structure at ambient conditions, while the B2 structure becomes more favorable either with decreasing crystal volume or with increasing Z (i.e. size) of the ligand atom. In CeP, an isostructural phase transition takes place at 71 kbar, and is found to originate from the f–electrons transferring their weight from localized to delocalized. At a larger pressure of 113 kbar a second phase transition takes place to the B2 structure. In CeAs, only one phase transition is observed, directly from the B1 structure with localized f–electrons to the B2 structure with delocalized f–electrons. In CeSb and CeBi a first phase transtion from B1 to (a distorted) B2 structure, both having localized f–electrons, is seen, at 70 and 88 kbars, respectively, while only at larger pressures the localization-delocalization transitions are found. Experimentally, only the first transitions have been observed. The magnetic structures of the cerium monopnictides is quite complicated. We do find the correct ($T = 0$ and $H = 0$) antiferromagnetic ground state of CeP and CeSb, but with rather small energy differences between various alternatives. This is in accord with the experimental fact that the Nèel temperatures of these compounds are rather small (~ 10 K), but is also a warning that really all relevant energy contributions should be considered, i.e. both spin-orbit coupling [7] and possibly a full-potential treament is called for, before reliable predictions regarding magnetic structures can be made.

Ongoing research applies the SIC-LSD formalism to a number of rare-earth systems, including Yb pnictides, CeB_6 and SmS.

References:

1. Z. Szotek, W. M. Temmerman and H. Winter, *The SIC-LSD Description of the $\gamma \rightarrow \alpha$ transition in Cerium*, Phys. Rev. Lett. **72**, 1244 (1994).

2. A. Svane, *Electronic Structure of Cerium in the Self-Interaction Corrected Local-Spin-Density Approxmation*, Phys. Rev. Lett. **72**, 1248 (1994).

3. A. Svane, *Electronic Structure of Cerium in the Self-Interaction Corrected Local-Spin-Density Formalism*, Phys. Rev. **B53**, 4275 (1996).

4. A. Svane, Z. Szotek, W. M. Temmerman and H Winter, *Theory of the Electronic and Magnetic Structure of Cerium Pnictides under Pressure*, Solid State Commun., to appear (1997).

5. W. M. Temmerman, A. Svane, Z. Szotek and H. Winter, *Applications of Self-Interaction Corrections to Localized States in Solids*, Proceedings of the Brisbane Density Functional

Theory Conference, Brisbane (Australia), July 1996.

6. A. Svane, Z. Szotek, W. M. Temmerman, J. Lægsgaard and H Winter, *Electronic Structures of Cerium Pnictides*, in preparation.

7. S. V. Beiden, W. M. Temmerman, Z. Szotek and G. Gehring, *Orbital moments in the fully relativistic self-interaction corrected band theory*, in preparation.

Highlight of Würzburg-Bristol Collaboration

Relativistic Approach to Dichroism in Superconductors

K. Capelle[†], E.K.U. Gross[†] and B.L. Gyorffy[‡]
[†]*Institut für Theoretische Physik, Universität Würzburg,*
Am Hubland, D-97074 Würzburg, Germany
[‡]*H.H. Wills Physics Laboratory, University of Bristol, Bristol, UK*

The collaboration between the groups of Prof. B.L. Györffy, Bristol, UK, and Prof. E.K.U. Gross, Würzburg, FRG, focuses on applying the relativistic theory of superconductivity to study dichroism in superconductors.

A system is said to exhibit dichroism if the absorption of light depends on its polarization [1]. Usually dichroism occurs if time reversal symmetry is broken through external or internal ('exchange') magnetic fields. The former case corresponds to the Faraday or Kerr effect, depending on whether it is observed in transmission or reflection, while the latter case is referred to as spontaneous dichroism. Instead of broken time reversal symmetry, dichroism can also result from lack of inversion symmetry. In normal metals and ferromagnets these phenomena have been the subject of many theoretical and experimental investigations [1, 2]. For superconductors, on the other hand, very little is known about mechanisms and consequences of dichroism. The objective of the collaboration is to develop a systematic theory of dichroism in superconductors.

We use the Bogolubov-de Gennes (BdG) approach to inhomogeneous superconductors in magnetic fields [3], including relativistic effects [4], and employ perturbation theory to incorporate a variety of potential sources for dichroism. As a measure of dichroism we use the difference, $\Delta P = P_{LHP} - P_{RHP}$, in the power absorption of light with left-handed polarization (LHP) and right-handed polarization (RHP). ΔP is proportional to $\mathrm{Im}[\sigma_{xy}(\omega)]$, the imaginary part of the offdiagonal elements of the conductivity tensor [5] which govern all magneto-optical phenomena.

Recently the BdG equations were generalized to include relativistic effects on the single-particle level [4]. ¿From this generalization, the full form of the spin-orbit operator in superconductors is known to have offdiagonal elements involving the pair potential (anomalous spin-orbit coupling), in addition to the well-known diagonal spin-orbit terms which contain the lattice potential. We include the spin-orbit terms, as well as orbital currents and order parameter inhomogeneities via stationary perturbation theory.

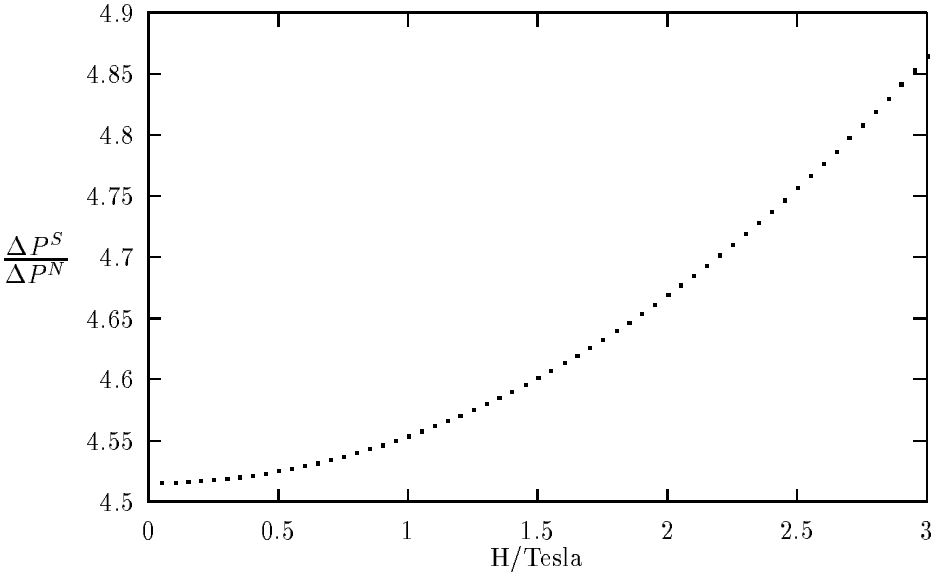

Figure 1: Dichroism ratio vs. magnetic field at $T = 3K$ for $\omega = 3meV$ and an energy gap at $T = 0$ of $2meV$.

Five distinct mechanisms which can give rise to a nonvanishing ΔP in superconductors were identified and interpreted in this way.

Mechanism 1: The conventional spin-orbit coupling (SOC) can, just as in normal metals, produce dichroism, provided that an (external or internal) magnetic field is present.

Mechanism 2: Anomalous spin-orbit coupling, too, can give rise to dichroism if magnetic fields are present. This term has a very different temperature behaviour compared to conventional SOC.

Mechanism 3: Orbital currents produced by $\mathbf{A}$, such as screening currents, can lead to a finite ΔP, without SOC. In normal metals this is usually smaller than the effects due to SOC. In superconductors, where the screening currents responsible for the Meissner effect are particularly large, this need not be the case any more.

Mechanism 4: Even in the absence of magnetic fields and SOC, $\mathbf{r}$-dependent pair potentials are a possible source of dichroism if they are either complex (i.e. break time reversal symmetry), or break inversion-symmetry. This is particularly interesting because it makes dichroism a potential tool to investigate unconventional order parameters.

Mechanism 5: A material which lacks a center of inversion already displays dichroism in the normal state. Such a material in general also displays dichroism in the superconducting phase.

What all mechanisms have in common, is that time reversal symmetry or inversion symmetry is broken, by magnetic fields, by the pair potential or by the lattice potential. Mechanisms 1 and 3, which were investigated thoroughly for normal metals, are present in superconductors as well. However, we find that they are strongly modified by the superconducting coherence. This is illustrated by the figures to be discussed below. Mechanisms 2 and 4 are special to superconductors and not present at all in the normal state.

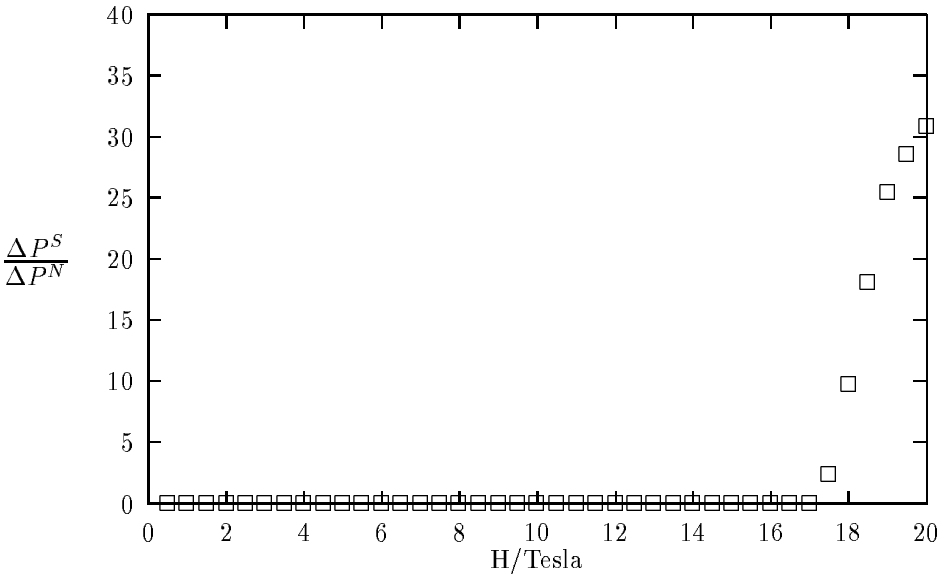

Figure 2: Same as in Fig. 1, but for $T = 0$ and fields up to the paramagnetic limit of superconductivity.

Those mechanisms requiring magnetic fields in the superconductor, namely 1, 2 and 3, cannot take place in the bulk of the material, as long as it is in the Meissner phase. They can be active in three different situations: (a) at surfaces, within the penetration depth, (b) in the vortex phase and (c) in superconductors displaying coexistence of magnetism and superconductivity. Mechanisms 1 and 2 are of relativistic origin. In particular, mechanism 2 constitutes the first potentially observable consequence of the anomalous spin-orbit coupling, predicted in [4].

Using simple approximations for the relevant matrix elements, we calculated ΔP for a model superconductor in which mechanism 1 is dominant. (Different model systems in which the other mechanisms dominate are currently under study.) In the plots we display the ratio of ΔP in the superconductor to ΔP in the normal conductor, $\Delta P^S/\Delta P^N$. This ratio is a direct measure for the interplay of relativistic symmetry breaking, due to mechanism 1, and superconducting coherence.

In Fig. 1 we plot $\Delta P^S/\Delta P^N$ versus the applied magnetic field. Both, numerator and denominator are almost linear functions of B and vanish for $B = 0$. Their ratio, however, is an increasing function of B because superconductors are more susceptible to magnetic fields than normal conductors. Repeating this calculation at $T = 0$, we find that the superconductor does not display dichroism for the fields in Fig. 1. This is physically reasonable, because at $T = 0$ a magnetic field will not produce spin polarization in a superconductor, since all electrons are paired. On the other hand it is known from normal state calculations that a finite spin magnetization is a necessary condition for SOC to produce dichroism. An alternative point of view is, that at $T = 0$ all paired electrons occupy mutually time conjugate states, so that the ground state is invariant under time reversal. Breaking this invariance, however, is mandatory for SOC induced dichroism.

In Fig. 2 we consider a superconductor with high upper critical field, H_{c2}. At zero temperature, we find, as before, $\Delta P^S \equiv 0$, until $B \approx 17.5T$. This is the field at which the Zeeman energy of

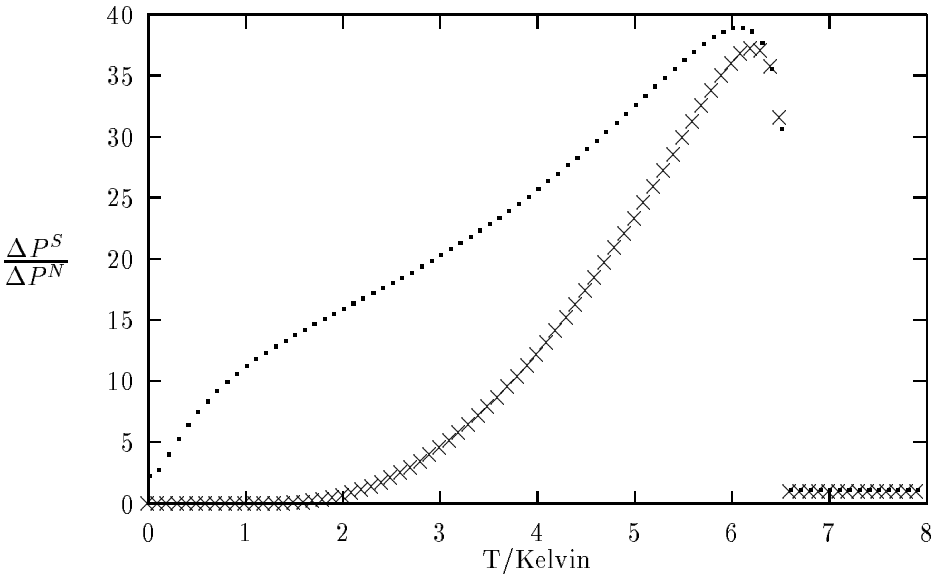

Figure 3: Dichroism ratio vs. temperature for $\omega = 4meV$ and $B = 0.1T$ (crosses) and $B = 17.5T$ (dots). T_c is at $6.6K$. Hebel-Slichter- and gap-enhancement are seen.

the electron spins equals the energy gap. At this strength the magnetic field can break Cooper pairs paramagnetically. Once there are unpaired electrons, the magnetic field will immediately produce a net spin magnetization (hence break time reversal invariance) and dichroism results. Interestingly, this effect could lead to a very direct experimental identification of paramagnetic limiting as the cause of the upper critical field.

In Fig. 3 we keep the field fixed and vary the temperature. Above T_c the ratio is unity. Right below T_c we find a drastic increase in dichroism in the superconductor [6]. This increase can be partly traced back to a Hebel-Slichter like effect, due to a novel combination of coherence factors. A second amplifying mechanism is due to the presence of the superconducting gap, [9, 10].

The second graph in Fig. 3 is for $B > \Delta$, i.e. for the paramagnetic limit of superconductivity. The peak below T_c is not affected much, but at $T = 0$ the curve for small fields goes to zero, while the curve for the paramagnetic limit approaches a finite value. This is in accordance with our discussion of Figs. 1 and 2.

In Fig. 4, finally, we display the frequency dependence of the absorption. There is an absorption edge at $\omega = 2meV$, which corresponds to the energy gap. This edge occurs because we considered only pair breaking processes [7]. The behaviour right above the edge is usually classified phenomenologically, according to the shape of the peak to be of type I or II [8], a classification which reflects the symmetry under time reversal of the perturbation (type I: odd, type II: even). The shape of the peak in Fig. 4 is of a mixed type, reflecting the fact that our model contains two perturbations, the polarized light (which is odd under time reversal) and the SOC (which is even).

The various plots demonstrate that even in the simple model many characteristics of the physics of dichroism and of superconductivity can be found. The exact numbers depend, of course, on the detailed parameters of the model. We believe, however, that the qualitative behaviour is

generic, and constitutes a definite signature of the SOC mechanism.

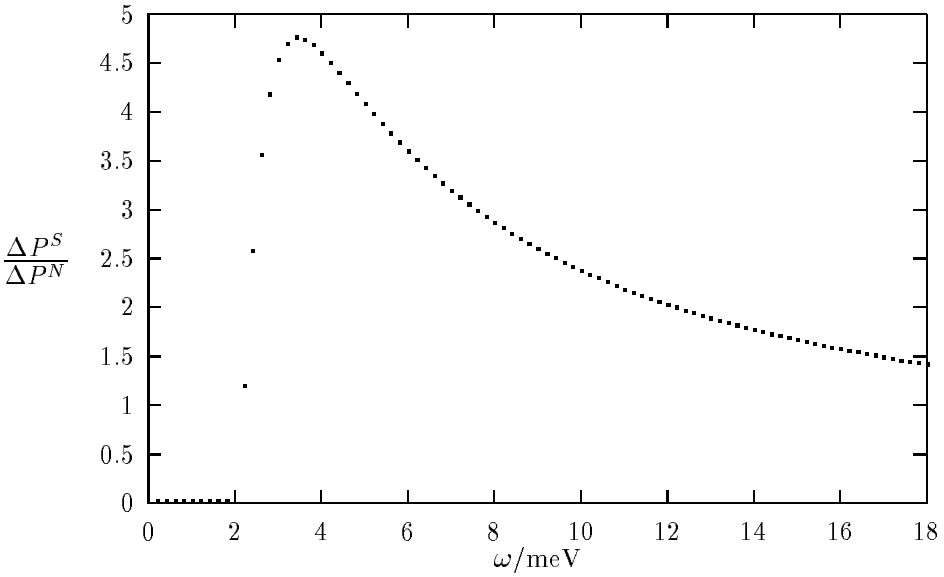

Figure 4: Dichroism ratio vs. frequency, at $T = 3K$ and for $B = 0.1T$. A mixed type I-II absorption edge at the gap energy of 2meV is present.

The above results have recently been submitted for publication [9]. A more detailed account of this work is currently being written [10].

References

[1] See the papers collected in *Spin-orbit influenced spectroscopies of magnetic solids*, eds. H.Ebert, G.Schütz, (Springer, Heidelberg, 1996).

[2] For a recent review see H. Ebert, Rep. Prog. Phys, (1996), in press.

[3] P.G. de Gennes, *Superconductivity of Metals and Alloys* (Benjamin, New York, 1966).

[4] K. Capelle, E.K.U. Gross, Phys. Lett. **A 198**, 261 (1995) and K. Capelle, E.K.U. Gross, to be submited.

[5] H. Bennett, E. Stern, Phys.Rev.**137**, A448 (1965).

[6] Below T_c the normal state calculation strictly speaking looses its meaning, but it still constitutes a convenient normalization, in particular, since the response of the *normal* conductor does not change much between $T = 0$ and $T = T_c$.

[7] Inclusion of single particle scattering produces a (generally small) additional absorption below the edge [8].

[8] M. Tinkham *Introduction to Superconductivity* (McGraw-Hill, New York, 1975).

[9] K. Capelle, E.K.U. Gross, B.L. Györffy, submitted for publication.

[10] K. Capelle, E.K.U. Gross, B.L. Györffy, in preparation.

On the semi-phenomenological quasi-particle spectra of high T_c superconductors

B.L. Gyorffy[†], Z. Szotek[‡], W.M. Temmerman[‡], O.K. Andersen[§], and O. Jepsen[§]

[†]*H.H. Wills Physics Laboratory, University of Bristol, Bristol, UK*
[‡]*Daresbury Laboratory, Warrington, WA4 4AD, UK*
[§]*Max-Planck-Institut für Festkörperforschung, Postfach 80 06 65, D-70506 Stuttgart, Germany*

Recently, a new semi-phenomenological approach to the problem of calculating the electronic structure in the superconducting state has been proposed [1]. It is based on a physically appealing, and very economical, parametrization of a phenomenological attractive interaction between the electrons afforded by the Density Functional Theory (DFT) of superconductivity [2] and the powerful LMTO-ASA methodology for solving self-consistent field problems for normal electrons [3, 4]. Preliminary calculations highlighted in the Ψ_k-Newsletter No. 13 (February 1996), indicated that the dramatic variation of the superconducting gap across the Fermi surface, as deduced from photoemission experiments, can be quantitatively reproduced with just one interaction constant. Here we report on some encouraging results of our first calculations of the specific heat [5] for YBCO, based on the same parametrization and without any further adjustable parameters.

The Kohn-Sham type Euler-Lagrange equations of the DFT for superconductors is of Bogoliubov-de Gennes, two-component, form and features the non-local pairing potential $\Delta(\mathbf{r}, \mathbf{r}')$. This latter quantity is related to the pairing amplitude $\chi(\mathbf{r}, \mathbf{r}')$, the order parameter of the problem, by the interaction kernel $\lambda^{(2)}(\mathbf{r}, \mathbf{r}'; \mathbf{r_1}, \mathbf{r'_1})$, which may be interpreted as an effective pairing potential. To make progress, it is expanded in terms of LMTO orbitals. In the present calculation these are those of the eight-band model of Andersen et al. [4]. The corresponding expansion coefficients are the parameters of the method. In the present calculation only one inequivalent expansion coefficient $\lambda_{\mu\mu';\mu\mu'}=\lambda_{\mu,\mu'}$, which describes the interaction of an electron in orbital labeled by μ and another in orbital μ' when the two electrons form a singlet, is kept and all the other coefficients were set equal to zero. In particular, the μ and μ' states were chosen to be $d_{x^2-y^2}$ orbitals on the nearest neighbour Cu sites of a CuO_2 bilayer. The corresponding λ was determined by the requirement that the calculated T_c agreed with experiments on optimally oxygenated YBCO. These were taken to imply that T_c=91.5 K.

In Fig. 1 we display the gap on the two main sheets of the Fermi surface as determined in the calculation described above. Evidently, it is highly anisotropic and it can be interpreted as having 'd-wave' symmetry [6]. Moreover, it agrees quantitatively as well as qualitatively with the gap deduced from photoemission experiments on optimally doped YBCO [7]. Given that

only the experimentally measured T_c was used to fit λ, this is an encouraging, if not altogether decisive, result.

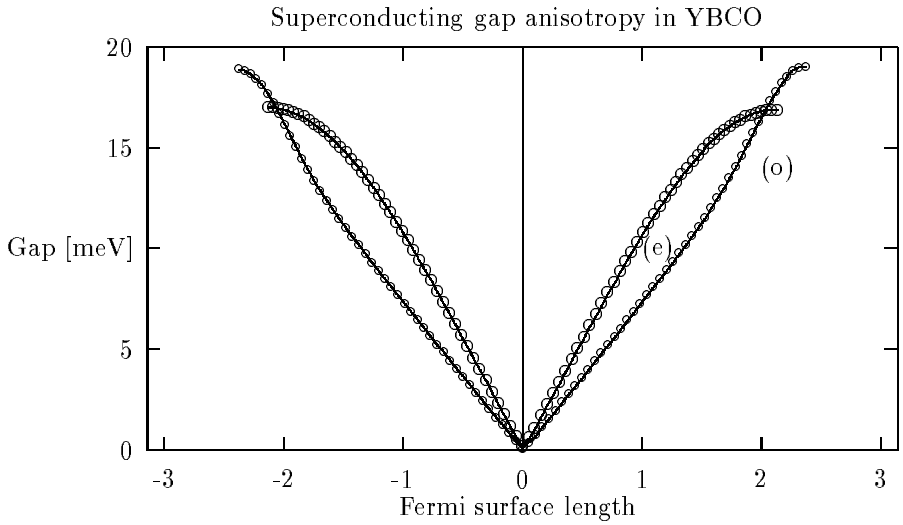

Figure 1: Superconducting gap for the nearest neighbour Cu $d-$Cu d interaction, as a function of Fermi surface length for even (e) and odd (o) sheets of the YBCO Fermi surface.

Having obtained the quasi-particle spectra in the superconducting state we can now calculate the specific heat without further adjustable parameters. The zero in $\Delta(\mathbf{k_F})$ on the (π,π) line implies a line of nodes on the full three-dimensional Fermi surface. This implies without numerical calculations, that at sufficiently low temperature the specific heat $C_v \approx T^2$, in dramatic contrast to exponential decay which is the prediction of the BCS model [6]. Whilst this power law behaviour is a general consequence of a line of nodes in $\Delta(\mathbf{k_F})$ on the Fermi surface, the coefficient of the T^2 contribution depends quantitatively on the quasi-particle spectra. Thus it is of interest to use $E_{\mathbf{k},\nu}$, which agreed with the photoemission experiments, to calculate C_v (T). The general formula for the specific heat due to independent quasi-particles is

$$C_v(T) = T\frac{dS}{dT} = \frac{1}{2}k_B\beta^2\sum_{\mathbf{k},\nu}(E_{\mathbf{k},\nu} + \beta\frac{\partial E_{\mathbf{k},\nu}}{\partial\beta})E_{\mathbf{k},\nu}sech^2(\frac{1}{2}\beta E_{\mathbf{k},\nu}). \tag{17}$$

Here S is the entropy, k_B is the Boltzmann constant, and β=1/k_BT. As is readily appreciated in the asymptotically small temperature T limit, the dominant contribution to the Brillouin zone integral in the above formula comes from the close vicinity of the node. We have developed a flexible method of integration which preferentially samples this relevant region. In the limit T $\rightarrow$ 0 we find

$$C_v(T) = 0.93(\frac{T}{T_c})^2(\frac{mJ}{molK}). \tag{18}$$

In measurements of the low temperature heat capacity for all the high T_c materials one finds large linear and cubic contributions which are not due to the superconducting electrons. Nevertheless, Moler et al. [8] have succeeded in extracting a quadratic contribution which in general supports

the emerging consensus [6] that the Cooper pairs in these materials have 'd-wave' internal symmetry. Moreover, they find

$$C_v(T) = 0.11T^2 = 0.91(\frac{T}{T_c})^2(\frac{mJ}{molK}) \tag{19}$$

which, to our pleasant surprise, is in good quantitative agreement with our semi-phenomenological calculations. Obviously, further work is required before the significance of these interesting developments are fully appreciated. Nevertheless, for the time being they point to the conclusion that whatever the physical pairing mechanism is, it operates between electrons of opposite spins on nearest neighbour Cu sites.

References

[1] W.M. Temmerman, Z. Szotek, B.L. Gyorffy, O.K. Andersen, and O. Jepsen, Phys. Rev. Lett. **76**, 307 (1996).

[2] L.N. Oliveira, E.K.U. Gross, and W. Kohn, Phys. Rev. Lett. **60**, 2430 (1988).

[3] O.K. Andersen, Phys. Rev. B **12**, 3060 (1975).

[4] O.K. Andersen, A.I. Lichtenstein, O. Jepsen, and F. Paulsen, J. Phys. Chem. of Solids, **56**, 1573 (1995).

[5] B.L. Gyorffy, Z. Szotek, W.M. Temmerman, O.K. Andersen, and O. Jepsen, in preparation.

[6] J.F. Annett, Adv. Phys. **39**, 83 (1990).

[7] J.M. Harris et al., Phys. Rev. B **54**, 15665 (1996).

[8] A.K. Moler et al., Phys. Rev. B **73**, 2244 (1994).

Highlights of Cambridge Collaborations in the Network

The active sites of microporous (zeolite) solid acid catalysts

Volker Heine and Rajiv Shah

TCM, Cavendish Laboratory, Cambridge, UK

The calculations described here were done in collaboration with Drs. J. Gale and M.C. Payne, connecting with the Highlight of 1995 reported by Dr. E. Nusterer et al. (Vienna) and the research on zeolite flexibility by Dr. A. Bieniok (Frankfurt), and benefiting from discussions with Prof. J. Sauer (Berlin).

As is well known, zeolites are microporous structures consisting of SiO_4 and $AlO_3(OH)$ tetrahedra joined into a three-dimensional framework by the shared oxygen atoms at the corners. They are important chemicals for various purposes, one of which is the catalytic activity of what are called Bronsted acid sites. At an aluminium containing tetrahedron, the extra proton needed for charge balance is attached to one of the four oxygens. It is available for creating a hydrogen bond to an adsorbed molecule, or for transfer to the molecule thus hydrogenating it. In the latter case it may result in splitting off an -OH group from the adsorbed molecule in the form of a water molecule.

The calculations were for the zeolite chabazite containing a methanol molecule in each unit cell. Chabazite has 36 atoms per unit cell, and contains rings of 8 tetrahedra (8-rings).

The first finding was that there are substantial differences amounting to 15 kJ/mol between the binding energies of the proton to the four sites, much larger than kT at ambient temperatures. We already see here the importance of the specific structure of the zeolite. A zeolite's structure is important in making it catalyse very specific reactions and not others, referred to as selectivity.

It was found that the methanol molecule is not physisorbed, as had been suggested by some previous cluster calculations. It is chemisorbed held by two hydrogen bonds. The proton from the Bronsted acid site is transferred to the methanol molecule, apparently without any energy barrier, forming an -OHH group at its end. This forms two hydrogen bonds to two oxygen atoms of the zeolite framework, with H-O distances of 1.38 $\AA$ and 1.54 $\AA$ respectively. The first of these is particularly close, indicating a very strong hydrogen bond, which explains the large hydroxyl stretching frequency shifts observed in the infrared spectrum. The molecule then lies snugly within the 8-ring, presumably held additionally by electrostatic and Van der Waals forces to the ring structure.

A similar calculation was carried out for a methanol molecule in a sodalite framework, the simplest model of a zeolite. It only has 6-rings which are not large enough to accommodate the molecule. The latter has to point into the body of the sodalite cage. In this situation the

calculations found the methanol only physisorbed, with no proton transfer from the Bronsted acid site of the framework to the molecule.

Clearly the energetics of proton transfer are finely balanced. The above and other results suggest that in ZSM-5 both protonated and unprotonated species may be present at ambient temperature. This is the commercial catalyst for methanol to gasoline, but it has a unit cell too large currently for ab initio calculations. It contains 10-rings, intermediate between the 8-rings of chabazite and the cage voids of sodalite referred to above.

Another issue arising from the calculations and being researched further is the role of zeolite flexibility. Zeolites are rather flexible structures, in fact they are extremely flexible in one or more very specific ways which are characteristic of the particular zeolite structures. One can expect such flexibility to be important in matching the shape of a corner of the framework to the need for bonding to the adsorbed molecule, and perhaps in letting go again in the chemical process.

The behaviour of gallium atoms in a grain boundary in aluminium

David Thomson and Volker Heine

TCM, Cavendish Laboratory, Cambridge, UK

This project (with Dr. M. C. Payne) is a collaboration with Prof. M. Finnis, started when he was in Stuttgart.

The project was motivated distantly by the phenomenon of grain boundary embrittlement, but understanding that is still some distance away since we do not know how impurity atoms behave in a grain boundary in a metal. In some cases they severely embrittle the metal, of which Ga is Al is a spectacular example, while in other cases they strengthen it.

The present study concerns various concentrations of Ga in one particular boundary, namely a $\Sigma = 11$ (113) tilt boundary in Al. Although it is only one specific case, a picture emerges of the energetics of Ga in different situations that we believe will have a wider applicability.

In this boundary the two grains really fit very well together. Of the two types of atomic site on the boundary, one (A) has 12 nearest neighbours as in bulk Al and the other (B) has 11. To be precise, the B site lies on the boundary plane and two A sites opposite to one another on either side. There are 44 atoms in a unit cell containing two boundaries with three atomic layers between them, and the system is always relaxed in the z direction taken perpendicular to the boundary plane. Various checks were carried out, e.g. the pure Al grain boundary energy compared with a previous calculation, and the heat of solution of Ga in bulk Al compared with experiment. The Al pseudopotential had previously been tested on the Al elastic constants, and the Ga pseudopotential had been tested and used in an extensive computational study of Ga.

The greatest possible care was taken with convergence in the number of k-points and correcting the energies to zero broadening at the Fermi level.

Ten calculations were carried out with between zero and 6 Ga atoms in each boundary placed on various sites on and near the boundary. The energy was compared with the same number of Ga atoms in bulk solid solution in Al. A regression analysis showed that Ga atoms are strongly attracted to the A sites (relative to bulk solid solution), but hardly at all to the B sites and to the C sites, the next adjacent on either side of the boundary. To be precise, a Ga atom is bound by 78 meV to an A site when the other A site of the pair is an Al atom. Another Ga atom is then attracted by 51 meV to the second A site of the pair.

To make sense of all this we have to look carefully at the local stresses as measured by the interatomic distances and the extension of the system perpendicular to the boundary (when fully relaxed), and at the changes in these as more Ga atoms are added to the boundary. In the pure Al boundary the B atoms are locally under some tension, balanced by an equal but opposite compression between the two A atoms in a pair. It is this compression which is relaxed by Ga atoms moving into the A sites. It is not that the A sites are particularly favourable for Ga atoms: rather the compression makes them unfavourable sites for the Al atoms.

The strange fact is that Ga in an (unstable computed) fcc structure has an atomic volume 10% larger than that of Al, and a Ga atom in bulk solid solution in Al expands the lattice by less than 1%. Hence Ga is certainly not a small atom. So how can it relax the tight A sites? The answer lies in the unusual structure of pure Ga with 7 near neighbours and the pseudopotential understanding of this fact. In metallurgy the sizes of atoms are the predominant determinant of alloy structures, but there used to be much discussion about how to define 'size': should it be based on the atomic volume or the nearest neighbour distance? The pseudopotential theory of the 1960's (and elaborated since then) shows that both are relevant, e.g. it is the interplay between them that accounts for the crystal structure of Ga. In an Al environment the Ga atom has a volume equal to that of an Al atom, but a hard-core radius determining the nearest neighbour distance smaller than that of Al. (This point is verified by calculating the restoring force constants for a Ga atom in bulk Al solid solution which are found to be weakened.) Thus in the A sites, Ga atoms are quite happy with the unusually short nearest neighbour distance between the pair of A sites. This picture is further supported by a calculation of the energy barrier for migration of the grain boundary, which involves short displacements by two A atoms each squeezing through a hole between three other atoms. The energy barrier is halved if the moving atoms are Ga, compared with Al, because again their smaller hard-core radius allows them to squeeze by more easily.

Other grain boundaries appear to be considerably less well fitting than the one studied here. We may therefore expect even stronger local compressions at some sites, which will therefore be even more attractive to Ga atoms. It remains to apply this principle to the behaviour of dislocations near the boundaries leading to embrittlement.

Highlights of Jülich-Vienna Collaboration

Transition-Metal Silicides for Electronic Devices

G. Bihlmayer *(Uni. Wien)*, S. Blügel *(Forschungszentrum Jülich)*,
and R. Podloucky *(Uni. Wien)*

Transition-metal (TM) silicides are widely used in very large scale integrated microelectronic and optoelectronic devices. The large variety of applications are due to a large variability in the electronic structure due to numerous different compounds and their match to a silicon-based technology. Most of these compounds are conductors. Some of them are used as interconnects, wires and contacts ($CoSi_2$ and $FeSi_2$). Some of them are semiconducting and are used for example as infrared sensors in infrared cameras. In order to build TM silicide structures at the Si wafer several techniques have been developed. One is the epitaxial growth of TM silicides on Si, an other one is TM ion implantation into Si followed by tempering which leads to buried TM silicides structures. With the rise of the glasfiber technology, it becomes necessary to match the silicon technology to the optoelectronic suitable for this technology. On demand is a silicide with a direct band-gap of 0.8eV with a large oscillatory strength. Motivated by the many material problems, last year the Vienna group and S. Blügel from Jülich teamed up to perform *ab initio* calculations of the electronic structure using the FLAPW method based on density functional theory in the local density approximation to look at several of the above problems.

(i) **$CoSi_2$/Si interface**:
First as a step towards understanding of the TM silicide/Si interface we investigated the clean $CoSi_2(110)$ surface [1], studying the electronic structure and surface relaxation effects. As a second point, it was found that the $CoSi_2$ grown on Si(100) shows a c(2×2) reconstruction, and it was not clear whether this reconstruction is due to the termination of the $CoSi_2$ surface by Co or Si. Recently carried out voltage dependent scanning tunneling microscopy (STM) experiments found that certainly both, the Co as well as the Si atoms terminate the $CoSi_2$, but due to the lack of chemical resolution of the STM, it was not clear which of the atoms are Co or Si. Calculating the STM image on the basis of the Tersoff-Hamann model [2] and comparing the theoretical images with the experimental ones led to the identification of the atom types.

(ii) **Buried layers of $FeSi_2$**:
Nowadays one is able to grow buried layers of $FeSi_2$ by ion-beam synthesis. The problem is that $FeSi_2$ exists in at least two phases: (a) the $\alpha-$ (high temperature) phase of $FeSi_2$. In this phase $FeSi_2$ is metallic. (b) the $\beta-$ (low temperature) phase, which is semiconducting with a band gap of 0.8 eV. A metastable $\gamma-$ phase was also found which is metallic and crystallizes in the CaF_2 structure. We found a strong influence of the crystallographic parameters on the size of the gap and, indeed, the transformation from $\gamma-$ to $\beta-$phase $FeSi_2$ can be viewed as an opening of a band gap due to a Jahn-Teller-like distortion. The basic problem is, that it is not *a priori* clear, which silicide is formed for a particular process condition. The electronic structure of the buried silicide was investigated by a novel technique called soft x-ray emission spectroscopy. We calculated the electronic structure of $\alpha-FeSi_2$ and $\beta-FeSi_2$ with and without core-hole and compared them with the experimental data [3] to unambiguously identify which

phase was formed.

(iii) **TM silicide for the optoelectronics**:
Most investigated silicides show metallic conductivity. An exception is for example $CrSi_2$, which has 14 valence electrons per formula unit. Most semiconducting TM silicides show a hybridization gap in the d-band region of the TM atoms. Since the band gaps are not direct gaps, the oscillator strength for d–d transitions is tiny and the d–bands rather flat and the mobility of the carriers rather low, most silicides have little potential for optoelectronic applications. On searching for new optoelectronic silicides we found the little investigated, but a large class of Nowotny-chimney-ladder silicides, characterized by the magic number of 14 valence electrons per formula unit. In this case the Fermi energy is located at the hybridization gap between p and d states. We suggested a promising new silicide for applications in the optoelectronic: Ru_2Si_3 [4]. We found a direct $p-d$ gap of 0.45 eV, opened by a strong Si (p) - Ru (d) hybridization and a p-band of high dispersion at the top of the valence band. Taking into account that the band gap is usually underestimated by LDA calculations, the true gap might be larger and may approach the 0.8eV needed for the glasfiber technology.

[1] D. Vogtenhuber and R. Podloucky, accepted for publication in Phys. Rev. B.
[2] B. Voigtländer, V. Scheuch, and H.P. Bonzel, S. Heinze and S. Blügel, submitted to Rapid Commun.
[3] S. Eisebitt, J.-E. Rubensson, M. Nicodemus, T. Böske, S. Blügel, W. Eberhardt, K. Radermacher, S. Mantl, G. Bihlmayer, Phys. Rev. B **50**, 18330 (1994).
[4] W. Wolf, G. Bihlmayer and S. Blügel, Phys. Rev. B **55** (7) (1997).